One electron oxidation of chromium *N,N*-bis(diarylphosphino)amine and bis(diarylphosphino)methane complexes relevant to ethene trimerisation and tetramerisation

Lucy E. Bowen, Mairi F. Haddow, A. Guy Orpen and Duncan F. Wass*

Complexes of the type [(diphosphine)Cr(CO)$_4$] (diphosphine = Ph$_2$PN(iPr)PPh$_2$, Ar$_2$PN(Me)PAr$_2$ or Ar$_2$PCH$_2$PAr$_2$ (Ar = 2-C$_6$H$_4$(MeO)) have been synthesised. In the solid state, these complexes show tight phosphine bite angles in the range 67.82(4)° to 71.52(5)° and the nitrogen atom in *N*-bis(diarylphophino)amine ligands adopts an almost planar (sp^2) geometry. All of the complexes are readily oxidised electrochemically or chemically to corresponding Cr(I) species. There is no evidence for coordination of the pendant ether group in derivatives with Ar = 2-MeO-C$_6$H$_4$ in either Cr(0) or Cr(I) species. Treatment of the [(diphosphine)Cr(CO)$_4$] complexes with [NO]BF$_4$ yields [(diphosphine)Cr(NO)(CO)$_3$]BF$_4$. Removal of CO ligands to generate an oligomerisation-active species is not observed with amine oxides but triethyl aluminium is effective in this role, and active catalysts can be produced. The use of weakly coordinating anions seems crucial in achieving oligomerisation catalysis.

Introduction

In recent years, several chromium catalysts have emerged capable of the selective trimerisation of ethene to 1-hexene *via* a distinctive metallacyclic mechanism.[1–3] In 2002, we reported catalysts based on chromium complexes of ligands of the type Ar$_2$PN(Me)PAr$_2$ (Ar = *ortho*-methoxy-substituted aryl group) with productivity figures over an order of magnitude better than previous systems.[2] This unprecedented performance led to interest both from a mechanistic viewpoint and in ligand structural modification,[3] the most significant subsequent development being the report from Bollmann and co-workers that relatively minor changes to ligand structure and reaction conditions can lead to ethene tetramerisation rather than trimerisation.[4]

Despite the growing importance of this catalyst family, the precise nature of active species remains to be defined, particularly with regard to the oxidation state of chromium through the catalytic cycle. The most compelling evidence to date comes from Bercaw and co-workers,[3a] and implicates a Cr(I)/Cr(III) manifold (Scheme 1). Treatment of the Cr(III) species, [CrPh$_3$(Ar$_2$PN(Me)PAr$_2$)] with one equivalent of H(Et$_2$O)$_2$BAF (BAF = B[3,5-C$_6$H$_3$(CF$_3$)$_2$]$_4$) yields an active catalyst together with benzene (from protonation of one phenyl ligand) and biphenyl (from subsequent reductive elimination of the other two). One can envisage a similar *modus operandi* for the more commonly used methyl aluminoxane (MAO) activator; in this case the cocatalyst acting as an alkylating agent to yield a chromium trimethyl intermediate, followed by abstraction of a methide ligand and reductive elimination of ethane.

Although the structural and reaction chemistry of these systems with Cr(III) centres is starting to be developed, Cr(I) complexes are by contrast unexplored. We became interested in

School of Chemistry, University of Bristol, Cantock's Close, Bristol UK BS8 1TS. E-mail: duncan.wass@bristol.ac.uk
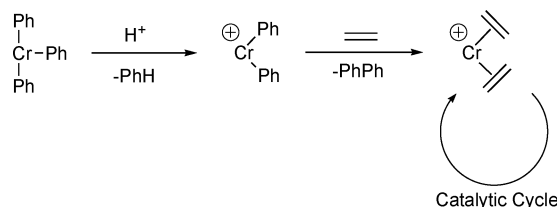
Scheme 1 Postulated mechanism of activation.

the possibility of accessing these important Cr(I) intermediates *via* one electron oxidation from Cr(0) complexes (see Scheme 2), particularly using analogues of well-known compounds of the type [(diphosphine)Cr(CO)$_4$]. Our objectives are to more fully explore the organometallic and coordination chemistry of such catalytic relevant species and ultimately develop MAO-free activation routes for catalysis.
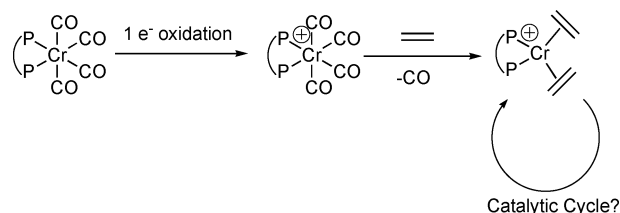
Scheme 2 One electron oxidation route to Cr(I) intermediates.

Results and discussion

Synthesis and structural characterisation of [Cr(CO)$_4$(diphosphine)] complexes 4–6

Our studies have focused on three ligand derivatives (Fig. 1): **1**, having an isopropyl N-substituent, demonstrates the best activity
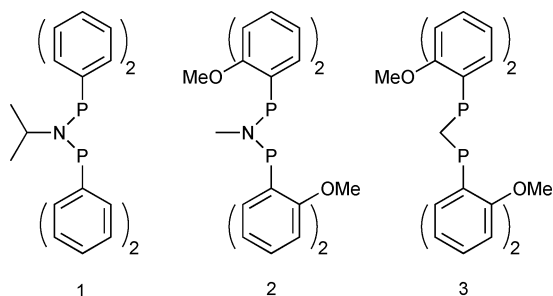
Fig. 1 Ligand derivatives.

and selectivity for ethene tetramerisation;[4] **2**, having *ortho*-anisyl P-substituents, has proved to be the most successful ligand for ethene trimerisation;[2] **3**, having a methylene chelate bridge, is inactive for oligomerisation reaction under the same conditions that **1** and **2** give good activity,[2] and we hoped that studying the fundamental chemistry of this ligand by way of comparison may provide insight to this surprising result.

Several synthetic routes to complexes of the general type $[Cr(CO)_4(Ar_2PN(R)PAr_2)]$ have been reported.[5] We found that simple reaction of ligand with $[Cr(CO)_6]$ under reflux in toluene proceeded most cleanly to give moderate (30–56%) yields of the desired products **4–6**. The carbonyl stretching region of IR spectra for these products is typical for $[M(CO)_4L_2]$ complexes, with often only three bands distinct because of overlapping peaks. Comparison of the data for **4** and **5** shows that, as expected, the presence of electron-donating OMe substituents of **2** results in this being the slightly more basic diphosphine (2005, 1919, 1888(br) cm^{-1} *vs* 2002, 1907, 1888, 1869 cm^{-1}). Data for complexes **5** and **6** reveal very similar stretching frequencies (2002, 1907, 1888, 1869 cm^{-1} *vs* 2002, 1906, 1888, 1860 cm^{-1}), despite **5** having the more electronegative nitrogen-based bridge. Clearly, the fact that this –PN(Me)P– backbone is almost planar (*vide infra*) with the delocalisation of the potential nitrogen lone pair over the chelate results in a more electron-rich diphosphine than might be first expected.

Crystals of **4**, **5** and **6** suitable for X-ray diffraction were grown from dichloromethane at −30 °C. The structure of a partially deuterated analogue of compound **5** has been previously reported.[6]

Compound **4** crystallises with two molecules in the asymmetric unit. The phenyl rings of the two crystallographically independent molecules adopt similar conformations (see Fig. 2, and Table 1), but the orientation of the *iso*-propyl group on the nitrogen is different (torsion angles P1–N1–C5–H5 = 30.4° and P3–N2–C36–H36 and 75.1°). This may be linked to the difference in the fold angle between the CrP$_2$ and P$_2$N planes in the two molecules: 10.9 and 4.9°. The pyramidality of the nitrogen atoms N1 and N2, (as measured by the sum of the angles around the nitrogen) is the same within error (356.9°), and implies sp^2 hybridisation at N. The Cr–CO bond lengths *trans* to the phosphorus atoms are slightly shorter than those *trans* to other carbonyls, consistent with the weaker *trans*-influence of the Cr–P bond.

The dichloromethane solvate of **5** crystallises with one molecule of the complex and one molecule of dichloromethane in the asymmetric unit (see Fig. 3, and Table 2). Neither the Cr–P bonds nor the Cr–CO bond lengths differ significantly from those in **4**, indicating that the effect of the methoxy groups on the Cr–P bond
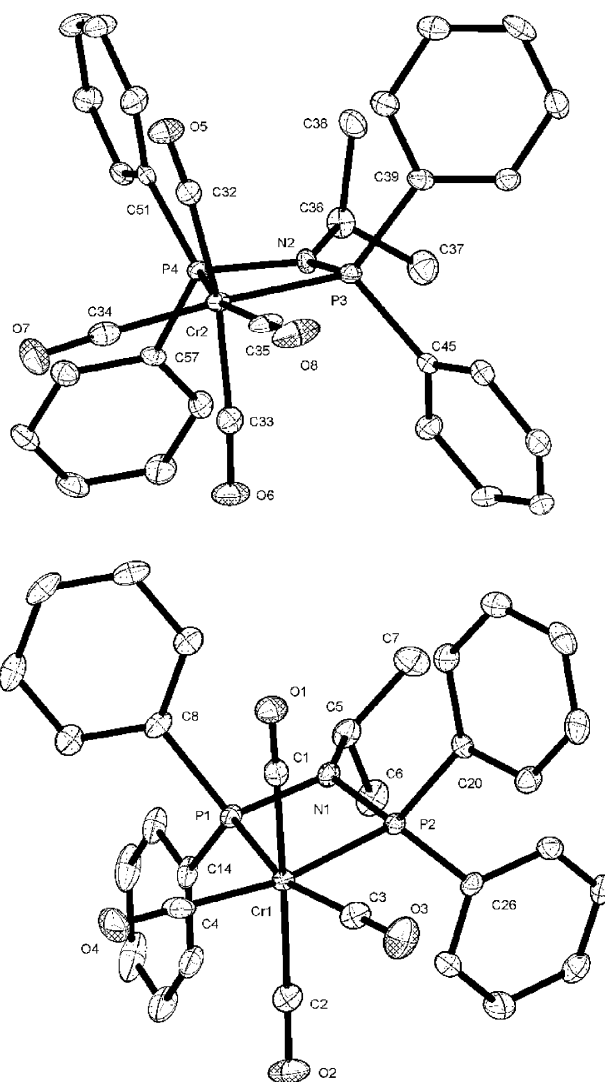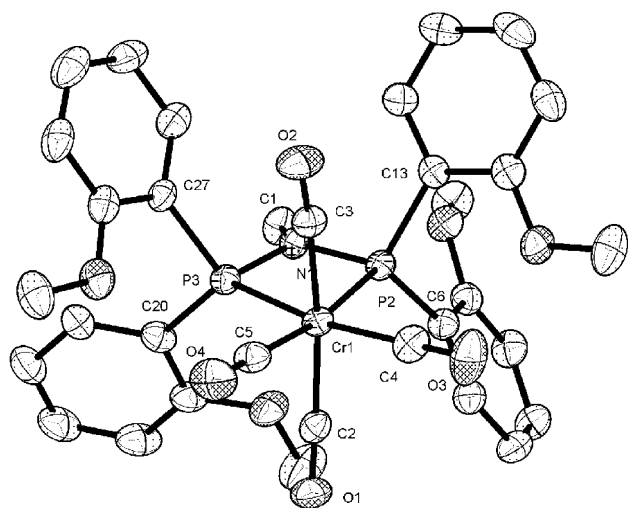

Fig. 2 Molecular structure and numbering scheme for $[Cr(CO)_4$-$(Ph_2PN(iPr)PPh_2)]$ **4** (Hydrogen atoms omitted for clarity; ORTEP plots created at 50% probability).

is small. However, the presence of the methoxy group results in a short intramolecular O1···O7 distance (3.02 Å). The carbonyl groups on the metal are bending away from the PNP ligand, but not to any greater extent than those in **4**, where the methoxy groups are not present. The Cr–P1–N1–P2 ring is almost flat, with a fold angle of 2.6°, and the nitrogen is again almost planar (sum of angles around nitrogen is 356.6°).

The dichloromethane solvate of **6** crystallises with two molecules of complex and two molecules of dichloromethane in the asymmetric unit (see Fig. 4, and Table 3). The crystallographically independent complex molecules adopt a similar (but not identical) conformation, each with an approximate mirror plane perpendicular to the plane of the Cr–P–C–P ring. The methoxy groups adopt a conformation where two on one face of the Cr–P–C–P ring point towards the metal, and two point away from it. The Cr–P–C–P rings are much less planar than the nitrogen equivalent, with fold angles of 16.9 and 15.8° in the two independent molecules, but the Cr–P bonds are much the same length as in those complexes with PNP ligands. The P–C bond is

Table 1 Selected bond lengths (Å) and angles (°) for **4**

Cr1–C1	1.878(3)	Cr2–C32	1.885(3)
Cr1–C2	1.891(3)	Cr2–C33	1.883(3)
Cr1–C3	1.862(3)	Cr2–C34	1.858(3)
Cr1–C4	1.858(3)	Cr2–C35	1.863(3)
Cr1–P1	2.3533(11)	Cr2–P3	2.3518(10)
Cr1–P2	2.3461(11)	Cr2–P4	2.3326(9)
P1–N1	1.714(2)	P3–N2	1.715(2)
P1–C8	1.822(3)	P3–C39	1.834(2)
P1–C14	1.833(3)	P3–C45	1.827(3)
P2–N1	1.712(2)	P4–N2	1.713(2)
P2–C20	1.828(3)	P4–C51	1.824(2)
P2–C26	1.827(3)	P4–C57	1.821(2)
P1–Cr1–P2	67.82(4)	P3–Cr1–P4	67.87(3)
P1–N1–P2	99.86(11)	P3–N2–P4	99.44(11)
N1–P1–Cr1	95.45(8)	N2–P3–Cr2	95.87(7)
N1–P2–Cr1	95.76(8)	N2–P4–Cr2	96.60(7)
N1–P1–C8	106.14(11)	N2–P3–C39	106.41(10)
N1–P1–C14	106.09(11)	N2–P3–C45	109.51(11)
C8–P1–C14	101.39(12)	C45–P3–C39	102.18(11)
N1–P2–C20	111.73(11)	N2–P4–C51	105.85(11)
N1–P2–C26	104.69(10)	N2–P4–C57	107.78(11)
C20–P2–C26	102.88(11)	C51–P4–C57	100.83(11)
Cr1–P1–C8–C9	−92.0(2)	Cr2–P3–C39–C40	161.29(16)
Cr1–P1–C8–C13	83.8(2)	Cr2–P3–C39–C44	−24.1(2)
Cr1–P1–C14–C15	−6.9(3)	Cr2–P3–C45–C46	88.2(2)
Cr1–P1–C14–C19	176.82(17)	Cr2–P3–C45–C50	−85.6(2)
Cr1–P2–C20–C21	−88.4(2)	Cr2–P4–C51–C52	18.0(2)
Cr1–P2–C20–C25	82.7(2)	Cr2–P4–C51–C56	−165.67(16)
Cr1–P2–C26–C27	−160.19(16)	Cr2–P4–C57–C62	−105.8(2)
Cr1–P2–C26–C31	28.3(2)	Cr2–P4–C57–C58	72.9(2)

Table 2 Selected bond lengths (Å) and angles (°) for **5**

Cr1–C2	1.892(3)
Cr1–C3	1.879(3)
Cr1–C4	1.868(3)
Cr1–C5	1.853(3)
Cr1–P1	2.3683(10)
Cr1–P2	2.3556(12)
P1–N1	1.710(2)
P1–C6	1.836(3)
P1–C13	1.833(3)
P2–N1	1.707(2)
P2–C20	1.844(3)
P2–C27	1.837(3)
P1–Cr1–P2	68.44(3)
P2–N1–P1	102.05(12)
N1–P1–Cr1	94.46(8)
N1–P2–Cr1	94.98(8)
N1–P1–C6	109.27(12)
N1–P1–C13	105.71(13)
C6–P1–C13	104.00(13)
N1–P2–C20	103.84(12)
N1–P2–C27	105.50(13)
C20–P2–C27	101.34(14)
Cr1–P1–C6–C7	164.6(2)
Cr1–P1–C13–C14	76.1(2)
Cr1–P2–C20–C21	−54.2(3)
Cr1–P2–C27–C28	−69.6(2)

Table 3 Selected bond lengths (Å) and angles (°) for **6**

Cr1–C2	1.875(3)	Cr2–C35	1.885(3)
Cr1–C3	1.882(3)	Cr2–C36	1.889(3)
Cr1–C4	1.845(3)	Cr2–C37	1.865(3)
Cr1–C5	1.868(3)	Cr2–C38	1.846(3)
Cr1–P1	2.3626(16)	Cr2–P3	2.3662(16)
Cr1–P2	2.3683(17)	Cr2–P4	2.3690(17)
P1–C1	1.848(3)	P3–C34	1.847(3)
P1–C6	1.824(3)	P3–C39	1.832(3)
P1–C13	1.825(3)	P3–C46	1.824(3)
P2–C1	1.846(2)	P4–C34	1.848(3)
P2–C20	1.824(3)	P4–C53	1.835(3)
P2–C27	1.823(3)	P4–C60	1.829(3)
P1–Cr1–P2	71.52(5)	P3–Cr2–P4	71.55(5)
P2–C1–P1	96.92(12)	P3–C34–P4	97.04(12)
C1–P1–Cr1	94.52(9)	C34–P3–Cr2	94.59(9)
C1–P2–Cr1	94.37(9)	C34–P4–Cr2	94.49(9)
C1–P1–C6	106.42(11)	C34–P3–C39	104.88(12)
C6–P1–C13	102.89(12)	C34–P3–C46	108.37(13)
C1–P1–C13	106.74(13)	C39–P3–C46	103.69(12)
C1–P2–C20	104.25(11)	C34–P4–C53	107.09(12)
C1–P2–C27	107.64(12)	C34–P4–C60	106.49(12)
C20–P2–C27	104.86(12)	C53–P4–C60	103.65(12)
Cr1–P1–C6–C7	152.44(17)	Cr2–P3–C39–C40	158.35(16)
Cr1–P1–C13–C14	66.9(2)	Cr2–P3–C46–C47	68.1(2)
Cr1–P2–C20–C21	−157.45(17)	Cr2–P4–C53–C54	−152.20(17)
Cr1–P2–C27–C28	−64.1(2)	Cr2–P4–C60–C61	−64.2(2)

Fig. 3 Molecular structure and numbering scheme for [Cr(CO)$_4$-(Ar$_2$PN(Me)PAr$_2$)] Ar = 2-C$_6$H$_4$(MeO) **5** (Hydrogen atoms omitted for clarity; ORTEP plots created at 50% probability).

longer than the P–N bonds in the cases above, and consequently the PCP angle is slightly smaller than the PNP angle. The bite angle (P–Cr–P) for the PCP ligand is slightly larger (at 71.5°) than those in the PNP complexes (which range from 67.5° to 68.4°).

Electrochemistry and one electron oxidation of 4–6

In general, complexes of the type [Cr(CO)$_4$(diphosphine)] can be oxidised to the Cr(I) species, albeit these 17 electron complexes are relatively unstable with respect to disproportionation (Scheme 3). For example, Connelly and co-workers have reported that the oxidation of [Cr(CO)$_4$(diphosphine)] (diphosphine = Ph$_2$PCH$_2$CH$_2$PPh$_2$, dppe or Ph$_2$PCH$_2$PPh$_2$, dppm) with NOPF$_6$ or AgClO$_4$ produces a 17 electron species [Cr(CO)$_4$(diphosphine)]$^+$ which is isolable but unstable. Cyclic voltammetry indicates that [Cr(CO)$_4$(dppm)] undergoes a reversible one electron oxidation.[7]

Cyclic voltammetry of **4**, **5** and **6** reveals a clean reversible one-electron oxidation in each case with $E_{1/2}$ of 0.79, 0.53 and 0.42 V vs SCE, respectively. As expected, the more electron rich complex **5** is more easily oxidised than **4**. Comparison of **5** and **6** shows that the bis(diarylphosphino)methane complex is more easily oxidised.
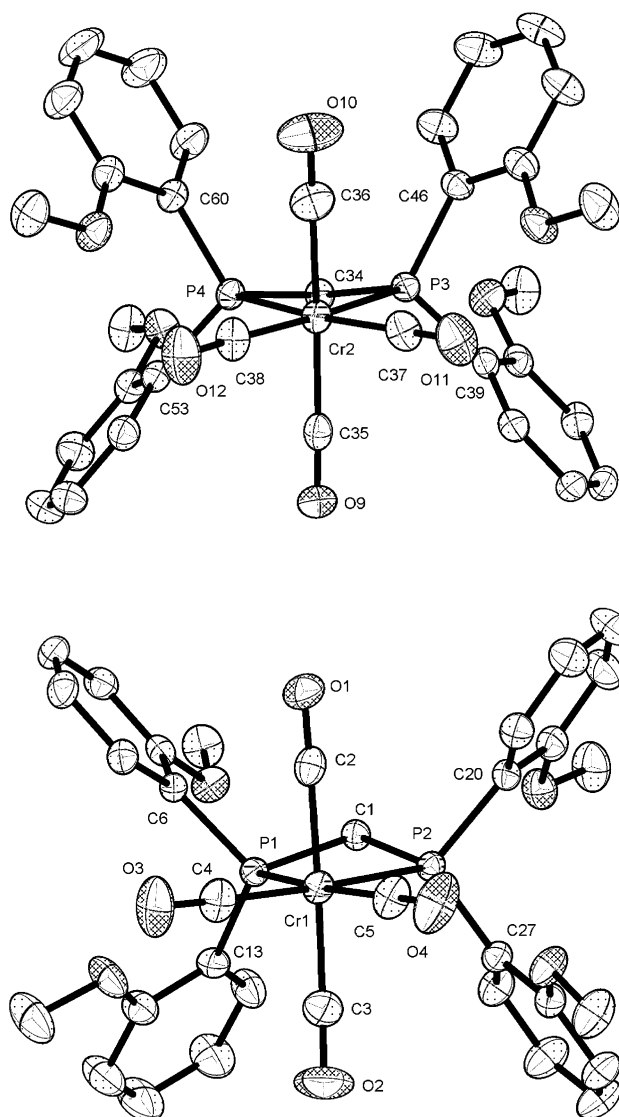
Fig. 4 Molecular structure and numbering scheme for [Cr(CO)$_4$-(Ar$_2$PCH$_2$PAr$_2$)] Ar = 2-C$_6$H$_4$(MeO) **6** (Hydrogen atoms omitted for clarity; ORTEP plots created at 50% probability).
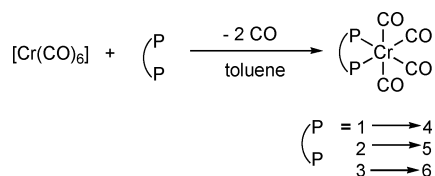
Scheme 3 Synthetic route to complexes **4–6**.

Chemical oxidation of **4–6** with acetyl ferrocinium tetrafluoroborate is also facile in each case, yielding cationic Cr(I) salts **7–9** (Scheme 4). Monitoring of the reactions by IR spectroscopy shows the expected shift to higher wavenumber for bands in the carbonyl region (for example, 2002, 1907, 1888, 1869 cm^{-1} to 2082, 2026, 1965 (br) cm^{-1} for **5** to **8**), consistent with less backbonding to CO ligands for the higher oxidation state species. It is noteworthy that the CO stretching bands observed for **8** and **9** are still those expected for complexes of the type [Cr(CO)$_4$L$_2$]; there is no evidence for coordination of pendant methoxy substituents.
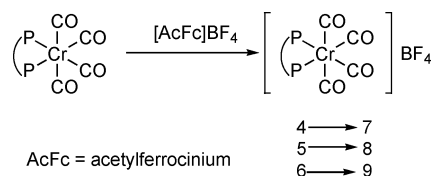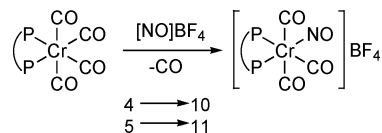

Scheme 4 Synthetic route to complexes **7–9**.

Although the Cr(I) complexes formed decompose slowly with time under a nitrogen atmosphere ($t_{1/2}$ *ca.* 24 h at room temperature) they are somewhat more stable than the analogous dppm or dppe complexes ($t_{1/2}$ *ca.* 4 h at room temperature). Monitoring this decomposition by IR spectroscopy shows the Cr(0) species **4–6** are re-formed, suggesting the previously observed disproportionation pathway is also operating in this case.

Synthesis and structural characterisation of [Cr(CO)$_3$(NO)(diphosphine)]BF$_4$ complexes 10–11

Reaction of complexes of the general formula [M(CO)$_4$-(diphosphine)] (M = Cr, Mo, W) with nitrosyl salts leads to either oxidation of the metal or formation of cationic M(O) nitrosyl complexes depending on the reaction conditions used.[7] As an alternative potential route to Cr(I) complexes, **4–5** were treated with one equivalent of [NO]BF$_4$ in MeOH/toluene according to Scheme 5. Characterisation data indicates that in fact cationic Cr(0) complexes of the general formula [Cr(CO)$_3$(NO)(diphosphine)]$^+$ are formed (**10–11**). This is consistent with the previous observation of the formation of analogous compounds with other diphosphine ligands under similar reaction conditions.

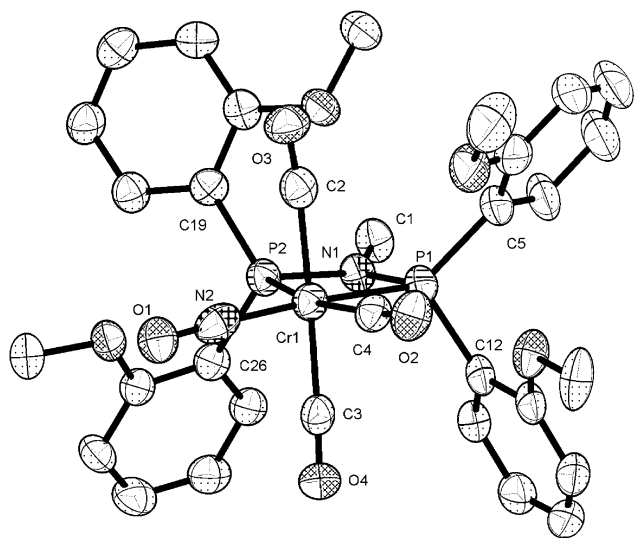**Scheme 5** Synthetic route to complexes **10–11**.

Crystals of **11** suitable for X-ray diffraction were grown from dichloromethane at −30 °C. The tetrafluoroborate salt **11** crystallises with one molecule of complex and anion in the asymmetric unit (see Fig. 5 and Table 4). The tetrafluoroborate anion is disordered over two orientations. The nitrosyl and carbonyl groups are ordered, with the nitrosyl *trans* to one of the phosphorus atoms. The Cr–NO bond [1.774(3) Å] is much shorter than the Cr–CO bond lengths, and is reflected in the longer *trans* Cr–P bond to this [2.4295(11) Å *cf.* 2.3816(9) Å *trans* to CO]. The Cr–P1–N1–P2 ring is again very flat; the fold angle is 2.4° with a near-planar nitrogen (sum of angles around N is 357.5°). The conformation of the methoxy groups differs from that in **5**, with three of the four methoxy groups pointing towards the metal. This again results in a short O3···O7 distance of 2.99 Å and a short C2···O7 distance of 2.88 Å.

CO ligand substitution and catalysis with complexes 4–9

There is no evidence for coordination of pendant methoxy groups in the complex family based on **2**, in contrast to the Cr(III) chemistry of this ligand.[3a,6] It seems that the carbonyl ligand of the complexes described to date are simply not sufficiently labile to be

Table 4 Selected bond lengths (Å) and angles (°) for **11**

Cr1–N2	1.774(3)
Cr1–C2	1.944(4)
Cr1–C3	1.928(4)
Cr1–C4	1.840(3)
Cr1–P1	2.4295(11)
Cr1–P2	2.3816(9)
P1–N1	1.700(2)
P1–C5	1.808(4)
P1–C12	1.815(3)
P2–N1	1.693(2)
P2–C19	1.816(3)
P2–C26	1.824(3)
P1–Cr1–P2	67.55(3)
P1–N1–P2	104.07(13)
N1–P1–Cr1	93.22(9)
N1–P2–Cr1	95.11(8)
N1–P1–C5	108.58(15)
N1–P1–C12	106.57(13)
C5–P1–C12	102.46(14)
N1–P2–C19	107.75(14)
N1–P2–C26	106.50(13)
C19–P2–C26	105.80(13)
Cr1–P1–C5–C6	17.4(3)
Cr1–P1–C12–C13	−70.5(3)
Cr1–P2–C19–C20	56.3(3)
Cr1–P2–C26–C27	66.5(2)

Fig. 5 Molecular structure and numbering scheme for [Cr(NO)(CO)₃-(Ar₂PN(Me)₂PAr₂)][BF₄] Ar = 2-C₆H₄(MeO) **11** (Hydrogen atoms and tetrafluoroborate counterion omitted for clarity).

displaced by this donor group. With this in mind, we attempted to remove one or more CO fragments from complexes **4–9** by treatment with 10 equivalents of amine oxides (pyridine *N*-oxide and trimethylamine oxide) or irradiation. In all cases, there was no evidence of CO displacement by IR spectroscopy. Perhaps not surprisingly given this observation, our attempts to use these Cr(I) complexes as catalytic precursors were unsuccessful. Treatment of **7–9** with 1 bar ethene at room temperature for 3 h yields no 1-hexene as determined by GC. Addition of 10 equivalents of pyridine *N*-oxide and trimethylamine oxide has no effect on this result. The use of more forcing conditions, 40 bar ethene at 60 °C, is also unsuccessful in the presence or absence of these amine oxides.

More success came from the use of triethyl aluminium as a CO ligand scavenger. Treatment of complexes **4–9** with 300 eq. of this reagent resulted in the loss of all peaks in the coordinated CO region of the IR spectrum and formation of a homogeneous orange–brown solution. To date we have been unable to characterise the species formed, and CO removal by action of the triethyl aluminium as a Lewis acid or alkylating agent are both possibilities. We have tested this method in catalytic ethene oligomerisation experiments (Table 5).

Potential catalysts were formed by treatment of complexes **4–6** with one equivalent of oxidising agent, followed by 300 eq. of triethyl aluminium. At 40 bar ethene pressure and 60 °C no activity is observed with acetyl ferrocenium tetrafluoroborate, *i.e.* complexes **7–9**. Unoxidised complexes **4–6** themselves are also inactive under these conditions. Reasoning that the tetrafluoroborate anion in these complexes may coordinate too strongly to the chromium centre or fluorinate the highly reactive species formed, we finally moved to a more stable and weakly coordinating anion, [B(C₆F₅)₄]⁻. Treatment of **4–6** with one equivalent of the clean and powerful one-electron oxidising agent [NAr₃][B(C₆F₅)₄] (Ar = 4-C₆H₄Br) gives complexes with identical IR spectra in the CO region to **7–9**. Following addition of triethyl aluminium, low oligomerisation activity is observed under the same conditions for complexes **4** and **5**. As previously observed with MAO activation, complex **4** gives both 1-hexene and 1-octene, complex **5** gives high selectivity to 1-hexene and complex **6** is inactive.

Conclusions

A range of low oxidation state chromium complexes of diphosphine ligands relevant to selective olefin oligomerisation catalysis have been prepared. The almost planar (sp²) geometry of nitrogen in *N*,*N*-bis(diarylphosphino)amine derivatives suggests delocalisation of the expected nitrogen lone pair over the ligand PNP

Table 5 Catalytic results

Compound[a]	Oxidising agent[b]	Productivity/g g⁻¹ h⁻¹	1-hexene (wt%)	1-octene (wt%)
4	[AcFc]BF₄	0	—	—
5	[AcFc]BF₄	0	—	—
6	[AcFc]BF₄	0	—	—
4	[NAr₃][B(C₆F₅)₄]	210	80	20
5	[NAr₃][B(C₆F₅)₄]	710	>99	0
6	[NAr₃][B(C₆F₅)₄]	0	—	—

[a] Conditions: 5 mmol compound, 1 eq. oxidising agent, 300 eq. triethyl aluminium, toluene diluent, 40 bar ethene, 60 °C; [b] AcFc = acetyl ferrocinium, Ar = 4-C₆H₄Br.

structure and leads to a relatively electron rich diphosphine. We propose this is likely to be a factor in the exceptional performance of these ligands in catalysis. Cr(I) complexes can be accessed *via* electrochemical or chemical oxidation; in derivatives with pendant ether groups there is no evidence for coordination of these groups, in contrast to higher oxidation state Cr(III) derivatives. Although the (lack of) lability of CO ligands must be taken into account, this provides indirect evidence for hemilabile behaviour in these ligands during catalytic cycles. Two factors seem important in generating active catalysts using this methodology. Firstly, efficiently removing the strongly bound CO ligands-to-date, an excess of triethyl aluminium is the only method we have found to be effective. A role for this reagent as a poison (oxygen and water) scavenger is also possible. Secondly, the counter-anion used must be stable and weakly coordinating, in parallel with early transition metal olefin polymerisation chemistry, $[B(C_6F_5)_4]^-$ is successful whereas BF_4^- is not. Of industrial relevance, although low productivity compared to MAO-activated systems is observed, this is offset by the much lower cost of triethyl aluminium compared to MAO. These results also give more weight to a Cr(I)/Cr(III) manifold during the catalytic cycle. We are now focussing on the synthesis of related complexes with potentially more labile ligands.

Experimental

General techniques

All procedures were carried out under an inert (N_2) atmosphere using standard Schlenk line techniques or in an inert atmosphere (Ar) glovebox. Chemicals were obtained from Sigma Aldrich or Fisher Scientific and used without further purification unless otherwise stated. All solvents were purified using an Anhydrous Engineering Grubbs-type solvent system. Ligands **1** and **2** were synthesised according to literature methods[2,4] and **3** was obtained in a method analogous to that reported for other bis(diarylphosphino)methane derivatives.[8] $[NAr_3][B(C_6F_5)_4]$ was synthesised according to the method of Nataro *et al.*[9]

Infra-red spectra were recorded on a Perkin-Elmer 1600 series FTIR Spectrometer in dichloromethane. Bands are characterised as strong (s), moderate (m), weak (w) and/or broad (br). NMR spectra were recorded on a JEOL ECP 300 spectrometer at 300 MHz (^{1}H) and 121 MHz (^{31}P) and a JEOL delta 400 at 200.6 MHz (^{13}C {^{1}H}), in deuterated solvent. ^{1}H and ^{13}C {^{1}H} NMR spectra are referenced chemical shifts relative to high frequency of residual solvent and ^{31}P NMR spectra are referenced relative to high frequency of 85% H_3PO_4. Microanalyses were carried out by the Microanalytical Laboratory of the School of Chemistry at the University of Bristol.

Synthesis of [Cr(CO)₄(diphosphine)] complexes 4–6

Synthesis of [Cr(CO)₄(Ph₂PN(iPr)PPh₂)] 4. Toluene (40 mL) was added to chromium hexacarbonyl, $[Cr(CO)_6]$, (350 mg, 1.6 mmol) and **1** (500 mg, 1.2 mmol) and the stirred mixture was heated under reflux for 48 h. The solution was cooled to 0 °C and filtered to remove excess $[Cr(CO)_6]$. Solvent was removed under reduced pressure and the product extracted into dichloromethane (10 mL). Methanol (20 mL) was added to precipitate the product,

which was isolated by filtration and dried *in vacuo* to yield a yellow solid (287 mg, 0.46 mmol, 44%). X-Ray-quality crystals were formed from a concentrated dichloromethane solution at 0 °C.

^{1}H NMR (CDCl₃, 300 MHz): $\delta = 0.62$ (d, 6 H, CH_3, $J_{HH} = 6.8$ Hz), 3.51 (sept, 1 H, CH, $J_{HH} = 7.0$ Hz), 7.19–7.90 (m, 20 H, ArH); ^{31}P NMR (CDCl₃, ref-H₃PO₄, 121 MHz): $\delta = 114$ (s); ^{13}C NMR (CDCl3, 67.9 MHz): $\delta = 1.1$ (s, CH_3), 23.6 (s, CH), 128.1 (d, $J_{CP} = 5.5$ Hz, CH), 128.5 (s, $J_{CP} = 5.5$ Hz, CH), 130.6 (s, CH), 132.0 (t, $J_{CP} = 15.9$ Hz, CH), 132.9 (d, $J_{CP} = 21.9$ Hz, CH), 127.2.(s, CP); IR (CH₂Cl₂): $v = 1889$ (s, br) (C≡O), 1919 (s) (C≡O), 2006 (s) (C≡O) cm⁻¹; Elemental Analysis: C₃₁H₂₇CrNO₈P₂ calcd (%) C 62.95, H 4.60, N 2.37, found C 62.60 H 4.62 N 1.90.

Synthesis of [Cr(CO)₄(Ar₂PN(Me)PAr₂)] Ar = 2-C₆H₄(MeO) 5. An analogous method to that for **4** was followed using chromium hexacarbonyl, $[Cr(CO)_6]$, (300 mg, 1.4 mmol) and **2** (500 mg, 0.96 mmol). The product was obtained as a yellow solid (380 mg, 0.56 mmol, 56%). X-Ray-quality crystals were formed from a concentrated dichloromethane solution at 0 °C.

^{1}H NMR (CDCl₃, 300 MHz): $\delta = 2.42$ (s, 3 H, CH_3), 3.59 (s, 12 H, OCH_3), 6.83–6.88 (m, 8 H ArH), 7.06–7.10 (m, 4 H, ArH), 7.24–7.32 (m, 4 H, ArH); ^{31}P NMR (CDCl₃, ref-H₃PO₄, 121 MHz): $\delta = 102$ (s); ^{13}C NMR (CDCl3, 75 MHz): $\delta = 51.6$ (s, CH_3), 55.0 (s, OCH_3), 110.7 (s, CH), 120.0 (t, $J_{CP} = 5.5$ Hz, CH), 131.6 (s, CH), 129.8 (t, CH), 133.1 (t, $J_{CP} = 11.0$ Hz), 159.7 (s, CP); IR (CH₂Cl₂): $v = 1869$ (s) (C≡O), 1888 (s) (C≡O), 1907 (s) (C≡O), 2002 (s) (C≡O) cm⁻¹; Elemental Analysis: C₃₃H₃₁CrNO₈P₂·1/2CH₂Cl₂ calcd (%) C 55.45, H 4.45, N 1.93, found C 55.17, H 4.85, N 1.88.

Synthesis of [Cr(CO)₄(Ar₂PCH₂PAr₂)] Ar = 2-C₆H₄(MeO) 6. An analogous method to that for **4** was followed using chromium hexacarbonyl, $[Cr(CO)_6]$, (170 mg, 0.60 mmol) and **3** (300 mg, 0.77 mmol). The product was obtained as a yellow solid (120 mg, 0.17 mmol, 28%). X-Ray-quality crystals were formed from a concentrated dichloromethane solution at 0 °C. ^{1}H NMR (CDCl₃, 400 MHz): $\delta = 2.33$ (s, 3 H, CH_3), 3.56 (s, 12 H, OCH_3), 6.65–6.78 (m, 4 H ArH), 6.85–6.95 (m, 4 H, ArH), 7.05–7.28 (m, 8 H, ArH); ^{31}P NMR (CDCl₃, ref-H₃PO₄, 121 MHz): $\delta = 19.9$ (s); ^{13}C NMR (CDCl₃, 100 MHz): $\delta = 22.8$ (s, CH_3), 55.1 (s, OCH_3), 110.6 (s, CH), 120.1 (dd. $J_{CP} = 5.4$ Hz, $J_{CP} = 15.4$ Hz, CH), 128.2, 129.0, 131.5 (s, CH), 133.7 (dd, $J_{CP} = 6.88$ Hz, $J_{CP} = 6.88$ Hz, CH), 160.2.(dd, $J_{CP} = 10.2$ Hz, $J_{CP} = 10.2$ Hz, CP), IR (CH₂Cl₂): $v = 1861$ (s) (C≡O), 1888 (s) (C≡O), 1906 (s) (C≡O), 2002 (s) (C≡O) cm⁻¹; Elemental Analysis: C₃₃H₃₀CrO₈P₂ calcd (%) C 59.29, H 4.52, found C 59.81, H 4.11.

Electrochemistry of 4–6

Electrochemical studies were carried out using an EG&G model 273A potentiostat linked to a computer using EG&G Model 270 Research Electrochemistry software in conjunction with a three-electrode cell. The working electrode was a platinum disc (1.6 mm diameter) and the auxiliary electrode a platinum wire. The reference was an aqueous saturated calomel electrode (SCE) separated from the test solution by a fine porosity frit and an agar bridge saturated with KCl. Solutions were 1.0×10^{-3} mol dm⁻³ in the test compound and 0.1 mol dm⁻³ in [NBuⁿ₄][PF₆] as the supporting electrolyte, the solvent used was CH₂Cl₂. Under these conditions, $E°$ for one electron oxidation of $[Fe(\eta^5-C_5H_5)_2]$ and

[Fe(η^5–C$_5$Me$_5$)$_2$], added to the test solutions as internal calibrants are 0.47 and −0.08 V, respectively. Unless specified all $E°$ values are at scan rate, v, of 200 mV s^{-1}.

Synthesis of [Cr(CO)$_4$(diphosphine)]BF$_4$ complexes 7–9

Synthesis of [Cr(CO)$_4$(Ph$_2$PN(iPr)PPh$_2$)]BF$_4$ 7. Complex 4 (20 mg, 0.034 mmol) and acetyl ferrocinium tetrafluoroborate (15 mg, 0.045 mmol) were dissolved in dichloromethane (5 mL) to give a dark purple solution. The Schlenk tube was covered with foil to reduce exposure of the reaction mixture to light. The solution was stirred at room temperature for 2 h and was monitored by infra-red spectroscopy. After 24 h, infra-red spectroscopy revealed approx. 50% of the product had converted back to 4. Attempts to isolate 7 by addition of diethyl ether (20 mL) resulted in precipitation of black intractable products.

IR (CH$_2$Cl$_2$): v = 1963 (s, br) (C≡O), 2033 (s) (C≡O), 2087 (s) (C≡O) cm^{-1}.

Synthesis of [Cr(CO)$_4$(Ar$_2$PN(Me)PAr$_2$)]BF$_4$ Ar = 2-C$_6$H$_4$(MeO) 8. An analogous method to that for 7 was followed using 5 (20 mg, 0.029 mmol) and acetyl ferrocinium tetrafluoroborate (12 mg, 0.036 mmol). After 24 h, infra-red spectroscopy revealed approx. 40% of the product had converted back to 5. Again, attempted isolation led to intractable products.

IR (CH$_2$Cl$_2$): v = 1965 (s, br) (C≡O), 2026 (s) (C≡O), 2083 (s) (C≡O) cm^{-1}.

Synthesis of [Cr(CO)$_4$(Ar$_2$PCH$_2$PAr$_2$)]BF$_4$ Ar = 2-C$_6$H$_4$(MeO) 9. An analogous method to that for 7 was followed using 6 (20 mg, 0.030 mmol) and acetyl ferrocinium tetrafluoroborate (12 mg, 0.036 mmol). Again, attempted isolation led to intractable products.

IR (CH$_2$Cl$_2$): v = 1962 (s, br) (C≡O), 2033 (s) (C≡O), 2084 (s) (C≡O) cm^{-1}.

Synthesis of [Cr(CO)$_3$(NO)(diphosphine)]BF$_4$ complexes 10–11

Synthesis of [Cr(CO)$_3$(NO)(Ph$_2$PN(iPr)PPh$_2$)]BF$_4$ 10. Complex 4 (72 mg, 0.15 mmol) and [NO][BF$_4$] (30 mg, 0.26 mmol) were dissolved in a toluene/methanol mixture (10 mL : 1 mL) to give a yellow solution and a yellow precipitate. The solution was stirred at room temperature for 1 h, during which time the precipitate dissolved. The solution was stirred for a further 2 h and then filtered and reduced in volume to about 5 mL under reduced pressure. Diethyl ether was added (20 mL) and the solution was stored at 0 °C overnight to give a yellow precipitate which was isolated by filtration and dried *in vacuo* (35 mg, 0.061 mmol, 41%).

IR (CH$_2$Cl$_2$): v = 1760 (s) (N≡O), 2022 (s) (C≡O), 2092 (s) (C≡O) cm^{-1}.; Elemental Analysis: C$_{30}$H$_{27}$BCrF$_4$N$_2$O$_8$P$_2$ calcd (%) C 60.71, H 4.59, N 4.72, found C 59.88, H 4.31, N 4.50.

Synthesis of [Cr(CO)$_3$(NO)(Ar$_2$PN(Me)PAr$_2$)]BF$_4$ Ar = 2-C$_6$H$_4$(MeO) 11. An analogous method to that for 10 was followed using 5 (140 mg, 0.20 mmol) and [NO][BF$_4$] (50 mg, 0.40 mmol). A yellow microcrystalline product was isolated (73 mg, 0.095 mmol, 47%). X-Ray crystals were formed from a 1 : 1 v/v dichloromethane/hexane solution at 0 °C.

IR (CH$_2$Cl$_2$): v = 1755 (s) (N≡O), 2024 (s) (C≡O), 2091 (s) (C≡O) cm^{-1}; Elemental Analysis: C$_{33}$H$_{31}$BCrF$_4$N$_2$O$_8$P$_2$ calcd (%) C 49.76, H 4.05, N 3.63, found C 49.83, H 4.45, N 3.79.

Removal of CO ligands

Attempted reaction with amine oxides. The same general procedure was repeated for all compounds 4–9 using both trimethyl-*N*-oxide and pyridine-*N*-oxide, but is described here for complex 8. No evidence for CO removal or substitution was found in any case.

Complex 5 (20 mg, 30 μmol) and acetyl ferrocinium tetrafluoroborate (12 mg, 35 μmol) were dissolved with stirring in toluene (20 mL), yielding a purple solution of 8 as confirmed by IR spectroscopy. To this, a solution of freshly sublimed trimethylamine-*N*-oxide (38 mg, 0.5 mmol) in toluene (10 mL) was added. After stirring for 2 h at room temperature, IR spectroscopy indicated only the presence of 8 and trace quantities of 5. The solution was heated under reflux for 18 h but IR spectroscopy again indicated only approximately equal quantities of 8 and 5.

Reaction with triethyl aluminium. The same general procedure was repeated for all compounds 4–9 but is described here for complex 8. Complex 5 (20 mg, 30 μmol) and acetyl ferrocinium tetrafluoroborate (12 mg, 35 μmol) were dissolved with stirring in toluene (20 mL), yielding a purple solution of 8 as confirmed by IR spectroscopy. To this, a solution of triethyl aluminium in toluene (1.9 M, 300 eq.) was added. After *ca.* 1 min at room temperature, IR spectroscopy indicated no peaks in the CO region and an orange–brown solution was formed.

Ethene oligomerisation catalysis

At low pressure. The same general procedure was repeated for all compounds 4–9 using both in the absence or presence of trimethyl-*N*-oxide or pyridine-*N*-oxide, but is described here for complex 8.

Complex 5 (20 mg, 30 μmol) and acetyl ferrocinium tetrafluoroborate (12 mg, 35 μmol) were dissolved with stirring in toluene (20 mL), yielding a purple solution of 8 as confirmed by IR spectroscopy. To this, a solution of freshly sublimed trimethylamine-*N*-oxide (38 mg, 0.5 mmol) in toluene (10 mL) was added. The solution was degassed under reduced pressure and placed under an ethene atmosphere. The solution was stirred for 2 h at 70 °C. After this time, the solution was allowed to cool to room temperature and dilute hydrochloric acid (10%) added. The organic layer was collected and washed with water, then dried over magnesium sulfate. No oligomerisation products were detected by GC.

At elevated pressure without triethyl aluminium. Reactions were performed in parallel using a Baskerville 10 multicell autoclave. The same general procedure was repeated for all compounds both in the absence or presence of trimethyl-*N*-oxide pyridine-*N*-oxide, but is described here for complex 8.

Complex 5 (20 mg, 30 μmol) and acetyl ferrocinium tetrafluoroborate (12 mg, 35 μmol) were loaded into a reaction cell in an inert atmosphere glovebox. The autoclave was removed from the glovebox and toluene (4 mL) added. To this, a solution of freshly sublimed trimethylamine-*N*-oxide (38 mg, 0.5 mmol) in toluene (1.5 mL) was introduced *via* syringe. The reactor was closed, heated to 60 °C and pressurised to 40 bar with ethene. The reaction was stirred for 1 h. The reactor was allowed to cool to room temperature and the pressure was slowly released. Dilute

Table 6 Crystallographic data

Compound	4	5	6	11
Colour, habit	Pale yellow plate	Yellow block	Pale yellow block	Yellow block
Size/mm	$0.40 \times 0.40 \times 0.02$	$0.48 \times 0.30 \times 0.07$	$0.38 \times 0.28 \times 0.16$	$0.09 \times 0.04 \times 0.03$
Empirical Formula	$C_{31}H_{27}CrNO_4P_2$	$C_{34}H_{33}Cl_2CrNO_8P_2$	$C_{34}H_{32}Cl_2CrO_8P_2$	$C_{32}H_{31}BCrF_4N_2O_8P_2$
M	591.48	768.45	753.44	772.34
Crystal system	Triclinic	Triclinic	Triclinic	Monoclinic
Space group	$P\bar{1}$	$P\bar{1}$	$P\bar{1}$	$P2_1/n$
a/Å	10.795(2)	10.850(2)	11.807(9)	11.398(2)
b/Å	15.430(3)	13.509(3)	17.767(11)	19.022(4)
c/Å	17.984(4)	13.657(3)	17.847(9)	18.460(4)
α/°	90.51(3)	76.40(3)	80.50(6)	90
β/°	106.82(3)	67.08(3)	86.84(4)	101.33(3)
γ/°	95.17(3)	81.53(3)	74.80(6)	90
V/Å³	2853.7(10)	1788.6(8)	3563(4)	3924.2(14)
Z	4	2	4	4
μ/mm⁻¹	0.55	0.609	0.609	3.748
T/K	100	173	173	100
Reflections: total/independent/R_{int}	32614/13018/0.0429	18942/8213/0.0526	37832/16293/0.0295	29906/7312/0.0980
Final R_1	0.0515	0.0512	0.0472	0.0480
Largest peak, hole/e Å⁻³	0.551, −0.350	1.219, −0.688	1.015, −1.151	0.445, −0.314

hydrochloric acid (10%) was added, the organic layer collected and washed with water, then dried over magnesium sulfate. No oligomerisation products were detected by GC.

At elevated pressure with triethyl aluminium. Reactions were performed using a very similar general procedure to that described above only the required amount of triethyl aluminium (1.9 M solution in toluene) was added after the addition of the required oxidising agent. Oligomerisation products were detected by GC; quantified using mesitylene as a standard.

X-Ray crystallography

X-Ray diffraction experiments on the dichloromethane solvates of $5\cdot CH_2Cl_2$ and $6\cdot CH_2Cl_2$ were carried out at 173 K on a Bruker SMART diffractometer and an experiment on **4** was carried out at 100 K on a Bruker SMART APEX diffractometer, both using Mo-Kα X-radiation ($\lambda = 0.71073$ Å). A Bruker PROTEUM diffractometer using Cu-Kα radiation ($\lambda = 1.54157$ Å) was used for $11\cdot(CH_2Cl_2)$. All experiments were performed using a single crystal coated in paraffin oil mounted on a glass fibre.[10a] All three diffractometers used a CCD area detector and intensities were integrated[10b] from several series of exposures, each exposure covering 0.3° in ω. Absorption corrections were based on based on multiple and symmetry-equivalent measurements using SADABS V2.10,[10c] and structures were refined against all F_o^2 data with hydrogen atoms riding in calculated positions, with isotropic displacement parameters equal to 1.5 times (methyl and hydroxyl hydrogen atoms) or 1.2 times (all other hydrogen atoms) using SHELXTL.[10d] Complex neutral-atom scattering factors were used.[10e] Crystal and refinement data are given in Table 6.

For **11**, the crystal also contained disordered solvent molecules which could not be resolved. This was modelled using SQUEEZE,[10f] which found the unit cell to contain an extra 166 electrons distributed over two voids, each of volume 317 Å³. This correlates well with having four extra molecules of dichloromethane per unit cell, one per asymmetric unit.

Furthermore, the BF_4^- unit was also disordered, and has been modelled as lying over two positions.

CCDC reference numbers 626712–626715.

For crystallographic data in CIF or other electronic format see DOI: 10.1039/b700559h

References

1 (a) J. T. Dixon, M. J. Green, F. M. Hess and D. H. Morgan, *J. Organomet. Chem.*, 2004, **689**, 3641; (b) D. F. Wass, *Dalton Trans.*, 2007, 816; (c) J. R. Briggs, *J. Chem. Soc., Chem. Commun.*, 1989, (11), 674; (d) W. K. Reagan, *Phillips Petroleum Company, EP 0 417 477*, 1991; (e) F. J. Wu, *Amoco Corporation, US Pat. 5811618*, 1995; (f) R. D. Köhn, M. Hauffe, G. Kociok-Köhn, S. Grimm, P. Wasserscheid and W. Keim, *Angew. Chem., Int. Ed.*, 2000, **39**, 4337.
2 A. Carter, S. A. Cohen, N. A. Cooley, A. Murphy, J. Scutt and D. F. Wass, *Chem. Commun.*, 2002, (8), 858.
3 (a) T. Agapie, S. J. Schofer, J. A. Labinger and J. E. Bercaw, *J. Am. Chem. Soc.*, 2004, **126**, 1304; (b) M. J. Overett, K. Blann, A. Bollmann, J. T. Dixon, F. Hess, E. Killian, H. Maumela, D. H. Morgan, A. Neveling and S. Otto, *Chem. Commun.*, 2005, **5**, 622.
4 A. Bollmann, K. Blann, J. T. Dixon, F. M. Hess, E. Killian, H. Maumela, D. S. McGuiness, D. H. Morgan, A. Neveling, S. Otto, M. Overett, A. M. Z. Slawin, P. Wasserscheid and S. Kuhlmann, *J. Am. Chem. Soc.*, 2004, **126**, 14712.
5 (a) M. S. Balakrishna, T. K. Prakasha and S. S. Krishnamurthy, *J. Organomet. Chem.*, 1990, **390**, 203; (b) J. Ellermann and W. Wend, *J. Organomet. Chem.*, 1983, **258**, 21.
6 S. J. Schofer, M. W. Day, L. M. Henling, J. A. Labinger and J. E. Bercaw, *Organometallics*, 2006, **25**, 2743.
7 P. K. Ashford, P. K. Baker, N. G. Connelly, R. L. Kelly and V. A. Woodley, *J. Chem. Soc., Dalton Trans.*, 1982, 477.
8 J. N. L. Dennett, A. L. Gillon, K. Heslop, D. J. Hyett, J. S. Fleming, C. E. Lloyd-Jones, A. G. Orpen, P. G. Pringle, D. F. Wass, J. N. Scutt and R. H. Weatherhead, *Organometallics*, 2004, **23**, 6077.
9 A. R. O'Connor, C. Nataro, J. A. Golen and A. L. Rheingold, *J. Organomet. Chem.*, 2004, **689**, 2411.

10 (*a*) *SMART diffractometer control software. SMART collections: version 5.054*, Bruker-AXS Inc., Madison, WI, 1997–1998; *SMART APEX collections: version 5.628*, Bruker-AXS Inc., Madison, WI, 2005; *PROTEUM collections: version 5.625*, Bruker-AXS Inc., Madison, WI, 1997–2001; (*b*) *SAINT V6.02 integration software* (**4**), Siemens Analytical X-ray Instruments Inc., Madison, WI, 1994; *SAINT V6.28* (**5**), Siemens Analytical X-ray Instruments Inc., Madison, WI, 2001; *SAINT V6.41* (**6**), Siemens Analytical X-ray instruments Inc., Madison, WI, 2002; *SAINT V7.06A* (**11**), Siemens Analytical X-ray Instruments Inc., Madison, WI, 2003; (*c*) *SADABS V2.10*, G. M. Sheldrick, University of Göttingen, 2003; (*d*) *SHELXTL program system version 5.1*, Bruker Analytical X-ray Instruments Inc., Madison, WI, 1998; (*e*) *International Tables for Crystallography*, Kluwer, Dordrecht, 1992, vol. C; (*f*) SQUEEZE, incorporated into PLATON, A. L. Spek, (2005), *A Multipurpose Crystallographic Tool*, Utrecht University, Utrecht, The Netherlands.